Eur. J. Mech. B - Fluids 20 (2001) 591–602

S0997-7546(01)01152-9/FLA

Self-preservation of rough-wall turbulent boundary layers

R.J. Smalley, R.A. Antonia, L. Djenidi *

Department of Mechanical Engineering, The University of Newcastle, New South Wales, 2308, Australia

(Received 18 May 2000; revised 1 November 2000; accepted 2 November 2000)

Abstract – It is proposed that all fully rough-wall boundary layers should satisfy self-preservation more closely than a smooth-wall boundary layer. Previous work has shown that the self-preserving forms of the momentum and turbulent kinetic energy equations for a zero pressure gradient turbulent boundary layer, at sufficiently high Reynolds number, require that the wall shear stress is constant with x, and the layer thickness increases linearly with x. Measurements in two rough wall boundary layers suggest these conditions are met without assuming a form for the mean velocity distribution, and are more likely to exist in a fully rough wall layer than a smooth wall layer. © 2001 Éditions scientifiques et médicales Elsevier SAS

1. Introduction

The concept of similarity solutions is well established for laminar boundary layers. Its importance is also well recognised from both experimental and mathematical points of view. Although the structure of a turbulent boundary layer differs significantly from that of a laminar layer, the concept of similarity or self-preservation has been widely used in turbulent boundary layers. Clauser [1,2] noted that similarity of the mean velocity profile across a turbulent boundary layer can be assumed with a fair degree of approximation. Clauser [1] singled out for study a class of simple equilibrium flows which he later [2] associated with a constant value of the parameter $\beta \equiv (\delta^*/\tau_w)(\mathrm{d}p/\mathrm{d}x)$, where δ^* is the displacement thickness, τ_w is the wall shear stress and $\mathrm{d}p/\mathrm{d}x$ is the mean streamwise pressure gradient. Analysis of self-preserving or equilibrium layers were subsequently made by Townsend [3–5] and Rotta [6] and several possible self-preserving turbulent boundary layers were considered, e.g., Mellor and Gibson [7], Herring and Norbury [8], Bradshaw [9], and Tani [10]. In a self-preserving layer, motions at different sections of the flow differ only in scales of velocity and length, for example the friction velocity $u_\tau \equiv (\tau_w/\rho)^{1/2}$ and the boundary layer thickness δ. The conditions these scales need to satisfy were tabulated by Rotta [6]; like Clauser [2], Rotta used u_τ and $\Delta \equiv \delta^* U_1/u_\tau$, where U_1 is the free stream velocity. When the wall is smooth, self-preservation is satisfied exactly only for the flow between converging planes. Strictly, self-preservation is not possible for a zero pressure gradient boundary layer (i.e. $U_1 = \text{const.}$); the experimental data (e.g., Osaka et al. [11]; Smith [12]) for a zero pressure gradient turbulent boundary layer over a smooth wall indicate that u_τ, or equivalently the local skin friction coefficient $C_f \equiv 2u_\tau^2/U_1^2$ continually decreases with x. For zero pressure gradient rough wall boundary layers, Rotta [6] and Tani [10] suggested that, with an assumed form for the mean velocity distribution, exact self-preservation was possible when the velocity and length scales meet specific conditions. Two particular types of boundary layers have been thought to exhibit self-preservation: the boundary layer over the so-called d-type roughness and the boundary layer over a specific k-type rough wall. The d-type roughness (consisting of transverse square

* Correspondence and reprints.
E-mail address: meld@alinga.newcastle.edu.au (L. Djenidi).

cavities, Perry et al. [13]; Wood and Antonia [14]; Tani [10]) is apparently characterized by $C_f = \text{const.}$ and a linear dependence with x of the so-called mean velocity profile 'error in origin', d_o. This has received some, though not unequivocal, experimental support ([13–16]). Rotta suggested that self-preservation can be achieved for flows over k-type roughnesses (i.e. those surfaces in which d_o does not show a linear dependence with x) and for which $dk/dx > 0$. Limited experimental data are provided by Liu and Huang [17] for this case, although they are insufficient to support self-preservation conclusively. Tani [10] noted that self-preservation exists in a boundary layer if Coles' profile parameter, Π does not vary with x.

A serious concern is that the classification of different rough surfaces is based solely on the effect the roughness exerts on the mean velocity, more specifically its distribution in the assumed logarithmic region. As yet, no cogent explanation has been advanced for the apparent structural differences between the particular d-type and the more common k-type roughnesses. However, both roughnesses exhibit substantial differences relative to a smooth wall. Djenidi et al. [16] presented detailed flow visualisations of the turbulent flow surrounding the d-type roughness while Krogstad and Antonia [18] showed differences with the wall normal components of the turbulence structure between two k-type roughnesses and a smooth wall. The visualisations of Liu et al. [19] suggested that fluid mixing increased over a transverse square bar roughness (k-type) with $p/k = 4$ (p/k is the streamwise pitch to roughness height ratio) compared with that over transverse square cavity roughnesses with $p/k = 2$. Furuya et al. [20] showed from pitot tube and pressure distribution measurements over a cylindrical rods-roughness that the greatest effect on the mean velocity distribution occurred when p/k was in the range 4 to 8.

In this paper, we propose a less constraining view of rough wall turbulent boundary layers in so far as no distinction is made between d-type and k-type roughnesses. A distinction is made only between smooth and fully rough walls. Fully rough walls are those in which the roughness elements protrude beyond the viscous sublayer. A feature of these boundary layers is the high Reynolds number, R_δ ($\equiv \delta u_\tau/\nu$ or Kármán number) that can be achieved relative to a smooth wall boundary layer. Also, not withstanding the difficulty of determining τ_w reliably in a rough wall layer, the rate of change of u_τ (or C_f) with x appears to be considerably smaller than that for a smooth wall layer.

The analysis in section 2 shows that a rough wall layer ought to be a better candidate for self-preservation than a smooth wall layer. Experimental details for a rod-roughness are given in section 3 and a comparison of methods used for estimating u_τ is provided in section 4. Support for self-presevation over two rough surfaces (*figures 1(a)* and *(b)*) is given in section 5. These surfaces consist of two-dimensional (2D) transverse square cavities and cylindrical rods, aligned in the spanwise direction and periodically spaced in the streamwise direction.

2. Self-preserving development of a turbulent boundary layer

The following self-preserving distributions for the mean velocity and Reynolds stresses are assumed [4,6]

$$\begin{aligned} U_1 - \overline{U} &= u_\tau f(\eta), \\ \overline{u^2} &= u_\tau^2 g_1(\eta), \\ \overline{v^2} &= u_\tau^2 g_2(\eta), \\ \overline{uv} &= u_\tau^2 g_{12}(\eta), \end{aligned} \tag{1}$$

where $\eta = y/\delta$, u and v are velocity fluctuations in the streamwise x and wall-normal y directions respectively; an overbar denotes time averaging. In a zero pressure gradient the scales u_τ and δ depend only on x.

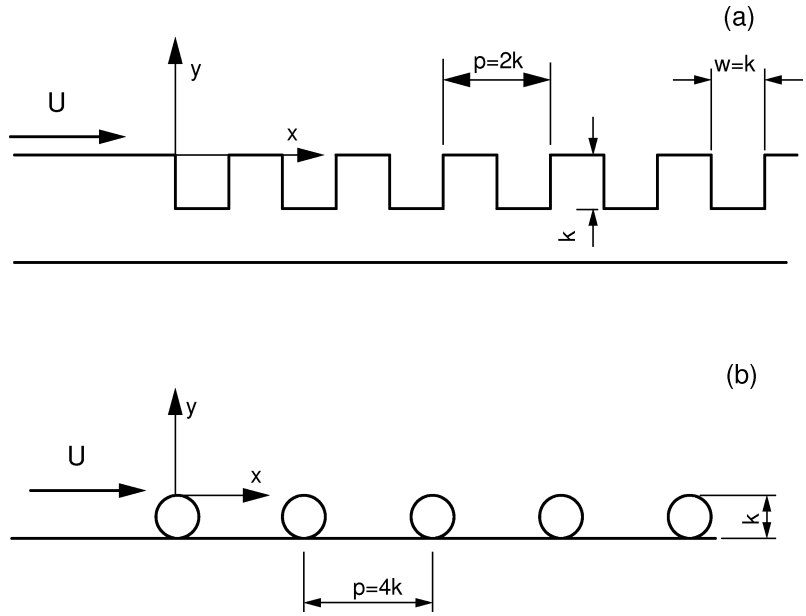

Figure 1. (a) transverse square cavity; (b) rod-roughness geometry.

Using the boundary layer approximation, the above distributions should satisfy the mean momentum equation

$$\overline{U}\frac{\mathrm{d}\overline{U}}{\mathrm{d}x} + \overline{V}\frac{\mathrm{d}\overline{U}}{\mathrm{d}y} + \frac{\mathrm{d}\overline{uv}}{\mathrm{d}y} + \frac{\mathrm{d}}{\mathrm{d}x}\left(\overline{u^2} - \overline{v^2}\right) = \nu\frac{\partial^2\overline{U}}{\partial y^2} \tag{2}$$

and the turbulent kinetic energy equation

$$\overline{U}\frac{\mathrm{d}\overline{(q^2/2)}}{\mathrm{d}x} + \overline{V}\frac{\mathrm{d}\overline{(q^2/2)}}{\mathrm{d}y} + \frac{\mathrm{d}}{\mathrm{d}y}\left(\frac{1}{2}\overline{q^2 v} + \frac{\overline{pv}}{\rho}\right) + \overline{uv}\frac{\partial\overline{U}}{\partial y} + \overline{\varepsilon} = 0, \tag{3}$$

where $\overline{q^2} = \overline{u^2} + \overline{v^2} + \overline{w^2}$ is twice the mean turbulent kinetic energy, $\overline{\varepsilon}$ is the mean turbulent energy dissipation rate and p is the pressure fluctuation. Substitution of equation (1) into (2) yields, after applying the continuity equation to find $\overline{V}$,

$$\begin{aligned} &-U_1\frac{\mathrm{d}u_\tau}{\mathrm{d}x}f + U_1\frac{u_\tau}{\delta}\frac{\mathrm{d}\delta}{\mathrm{d}x}\eta f' + u_\tau\frac{\mathrm{d}u_\tau}{\mathrm{d}x}\left\{f^2 + 2(g_1 - g_2)\right\} - \frac{u_\tau}{\delta}\frac{\mathrm{d}(u_\tau\delta)}{\mathrm{d}x}f'\int_0^\eta f\,\mathrm{d}\eta \\ &-\frac{u_\tau^2}{\delta}\frac{\mathrm{d}\delta}{\mathrm{d}x}\eta(g_1' - g_2') + \frac{u_\tau^2}{\delta}g_{12}' = -\nu\frac{u_\tau}{\delta^2}f', \end{aligned} \tag{4}$$

where a prime denotes differentiation with respect to η. The retention of the viscous term would require that the Kármán number remain constant (Rotta [6]); this is an overrestrictive constraint. If equation (4) is multiplied by δ/u_τ^2, the viscous term can be neglected if R_δ is large enough, a condition which is more readily achievable for a rough wall than a smooth wall layer. Results obtained over the rod-roughness, those of Hosni et al. [21] over a 3D roughness consisting of hemispherical elements and those of Ranga Raju et al. [22] over a gravel roughness all suggest that, at constant x, $\partial\delta/\partial U_1]_{\mathrm{rough}} > \partial\delta/\partial U_1]_{\mathrm{smooth}}$. Since nearly all rough walls are drag-augmenting surfaces, then $R_{\delta_{\mathrm{rough}}}$ should be greater than $R_{\delta_{\mathrm{smooth}}}$.

The coefficients of all other terms in (4) are independent of x if

$$\frac{\mathrm{d}\delta}{\mathrm{d}x} = \text{const.}, \tag{5}$$

$$u_\tau = U_1\sqrt{\frac{C_f}{2}} = \text{const.} \tag{6}$$

These conditions automatically satisfy the self-preserving form of the momentum integral equation. They also satisfy (3) if self-preserving forms for $\overline{q^2}$, $(\overline{q^2 v} + \overline{pv})$ and $\overline{\varepsilon}$ are written in a similar manner to (1). In arriving at (5) and (6), no assumptions were made regarding a particular shape of the mean velocity profile, e.g., a log-law with a prescribed wake function. However a remark should be made about these conditions. Based on Reynolds stress measurements obtained at relatively high Reynolds numbers, Krogstad and Antonia [18] showed that the distributions in equation (1) do not exhibit complete similarity over all wall surfaces. Hence the functions g_1, g_2 and g_{12} are more likely to depend on both η and a roughness geometry or roughness density parameter. The form that the latter may take is not known. The double dependence suggests that (1) may not be a sufficient condition for self-preservation; it may however, indicate approximate self-preservation over a particular wall surface.

Although numerous experiments have been performed over rough walls under zero pressure gradients, few have been undertaken with the specific objective of investigating the self-preservation of various rough wall turbulent boundary layers. Bandyopadhyay [23] concluded that both the transverse square cavity and a k-type roughness (sandgrain) in a transitional regime can achieve self-preservation. However self-preservation for the sandgrain roughness only occured after a sufficient streamwise fetch. Transitionally rough surfaces are those classified between hydraulically smooth and fully rough surfaces. This paper will focus on three boundary layer surfaces. Results from Osaka et al. [15] over a transverse square cavity roughness will be compared with those over a smooth wall (Smith [12]) and the present rod-roughness.

3. Experimental details

Measurements were made in an open-return blower tunnel, previously described in Krogstad et al. [24]. The boundary layer developed over a vertical wall of the tunnel working section and was tripped at the tunnel contraction by a 4 mm diameter trip rod followed by 170 mm of No. 40 grit sandpaper, both spanning the height of the working section. Immediately downstream of the sandpaper, the vertical surface of the working section was covered with a roughness comprising two dimensional cylindrical copper coated steel rods of diameter 1.6 mm. These spanned the full height and were placed at a streamwise pitch to roughness height ratio (p/k) of 4. Between 1.6 and 3.1 m (measured from the tunnel contraction exit) the mean pressure gradient was maintained to within 1% of the freestream dynamic pressure while the freestream turbulence intensity ranged between 0.4% and 1.2%.

The tunnel speed was nominally 10.1 ms^{-1} and the Reynolds number, $(R_\theta \equiv U_1\theta/\nu)$, over the extent of the measurements varied between 5 800 and 10 000, where θ is the momentum thickness. At $R_\theta = 10\,000$, the roughness Reynolds number, k^+, was about 60 (the superscript $+$ indicates normalisation by wall variables). For a 2D rough wall, the lower limit of k^+ for fully rough flow is 10 (Bandyopadhyay [23]). All results presented over the rod-roughness were measured with a X-wire probe operated by in-house constant temperature anemometers at an overheat ratio of 1.5. The wires were etched (from $d_w = 2.5$ μm Pt-10 Rh Wollaston wire) to an effective wire length l_w of about 200 d_w. The wires were separated by a nominal distance of 0.5 mm and had apex angles between 101°–107°. Calibration was carried out in the freestream before and after each profile using a fourth-order, least squares polynomial fit to velocity versus voltage data. If the mean velocity differed between the two calibrations by more than 2%, the data were rejected. The X-wires were yaw calibrated using

the method described in Browne et al. [25]. Measurements were carried out over a roughness element crest and the wall proximity distance was determined using a theodolite measure of the distance between the roughness element crest and the centre of the X-wire. The error associated with this method was approximately ± 0.1 mm ($y^+ \approx 3.6$). Data were acquired at a sampling frequency of either 12.6 or 16.0 kHz and low-pass filtered (cut off frequency $f_c = f_s/2$), using fourth-order-Butterworth filters. Sample times were between 26 and 40 s.

4. Estimation of u_τ

To test for self-preservation, an accurate estimate of u_τ is required. While for a smooth wall boundary layer, u_τ can be easily measured, it is less straight forward over a rough wall where τ_w ($\equiv \rho u_\tau^2$) receives contributions from the form drag, τ_p and viscous shear stress, τ_v, via $\tau_w = \tau_p + \tau_v$.

In the following, we compare various methods for obtaining u_τ over different surfaces. Osaka et al. [11,15] measured τ_w over a smooth wall and a transverse square cavity roughness respectively using a drag balance. Over the smooth wall, the resulting u_τ was within 2% of the value estimated from the momentum integral equation, viz

$$u_\tau^2 = U_1^2 \frac{\mathrm{d}\theta}{\mathrm{d}x} + \int_0^\delta \frac{\partial}{\partial x}\left(\overline{v^2} - \overline{u^2}\right) \mathrm{d}y.$$

Smith [12], also for a smooth wall, determined u_τ indirectly from the Clauser chart method. Over the same R_θ range ($4\,600 \leqslant R_\theta \leqslant 6\,200$), u_τ was in reasonable agreement with that of Osaka et al. [11]. The data of [12] (hereafter referred to as the smooth wall) will be used as reference in the present experiment, as it covers an R_θ range ($4\,900 \leqslant R_\theta \leqslant 10\,000$) equivalent to that of the two rough wall turbulent boundary layers.

A reasonable estimate of u_τ may be inferred from the Reynolds shear stress distribution. Over most wall surfaces at relatively high R_θ, a plateau of $-\overline{uv}$ exists at about $y/\delta \approx 0.2$ (see for example *figure 2*). If this plateau is assumed to correspond to a constant shear stress region (usually $y/\delta < 0.4$), the magnitude of $-\overline{uv}_{\text{plateau}}$ is then equivalent to u_τ^2. This method has been used extensively in atmospheric surface layer and rough wall investigations (e.g. [26,27]).

In the present experiment $-\overline{uv}]^{1/2}_{\text{plateau}}$ was used as an initial estimate for u_τ. This estimate is used to plot U^+ versus $\log(y^+ + d_0^+)$, a refinement of u_τ is then sought from a logarithmic least-squares fit to the data for the region between $y^+ > 50$ and $y/\delta \leqslant 0.15$. The modified Clauser chart method applied to the rough wall mean velocity profile assumes that part of the profile scales logarithmically. This method differs from that used by Tani [10] who optimised the fit for u_τ, d_0 and Π across the entire velocity profile. The value for $-\overline{uv}]^{1/2}_{\text{plateau}}$ in *figure 2* for each streamwise station shows that the least-squares fit within the inner region of the boundary layer adjusted u_τ by no more than 4%, this is well within the error for C_f estimated from $-\overline{uv}]^{1/2}_{\text{plateau}}$.

5. Comparison between rough and smooth walls

5.1. Conditions for self-preservation

Measurements over the rod-roughness were taken at 5 streamwise stations within the zero pressure gradient extent of the boundary layer. *Figure 3(a)* shows that δ^*, θ and δ increase approximately linearly with x. A similar result is observed for δ^* and θ over the transverse square cavity roughness (*figure 3(b)*) of Osaka et al. [15] and also for δ (not shown), as measured by Djenidi et al. [16] (see also [14]) over the same type of roughness. These results satisfy equation (5). However, *figure 3(c)* suggests that δ^*, θ and δ for a smooth

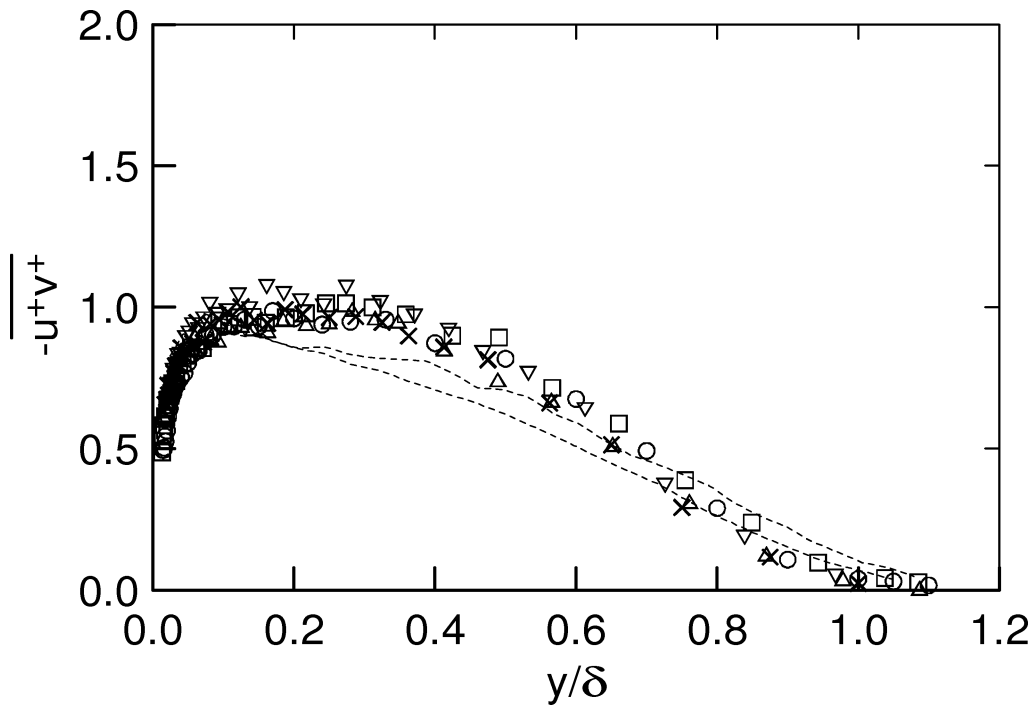

Figure 2. Reynolds shear stress for the rod-roughness and smooth wall. Rod-roughness: ▽, 1.6 m; ×, 2.0 m; △, 2.5 m; ○, 2.7 m; □. 3 m. - - - smooth wall [12]; lower line, $x = 1.1$ m; upper line, $x = 4.1$ m.

wall layer may also vary linearly with x. This highlights the difficulty of assessing self-preservation with (5). A more restrictive condition is $C_f = \text{const.}$ (or equivalently equation (6)) for a turbulent boundary layer in a zero pressure gradient. *Figure 4* shows that C_f is approximately constant over the transverse square cavity roughness while it decreases with x over the smooth wall [12]. Also shown are the data of [11], which exhibits a similar streamwise variation which agrees well with that of [12]. Over the rod-roughness, C_f decreases by approximately 2% over 2 m, compared with an 11% decrease over the smooth wall. These results indicate that self-preservation is better approximated in a fully rough wall layer than a smooth wall layer.

Further support for self-preservation over the rod-roughness is provided by the mean velocity defect, streamwise and normal Reynolds stresses and Reynolds shear stress distributions at 5 streamwise stations. The smooth wall distributions corresponding to 1.1 m and 4.1 m are at the extreme ends of the measuring range and are used for comparison. The collapse of the velocity defect distributions (*figure 5*) are equally reasonable for both surfaces suggesting that the mean velocity defect is not a very sensitive test of self-preservation. The Reynolds stresses for the rod-roughness and the smooth wall are shown in *figures 2* and *6*. There is negligible streamwise variation for $\overline{u^{+2}}$ over the rod-roughness compared with an increase in the magnitude of $\overline{u^{+2}}$ between $x = 1.1$ and 4.1 m for the smooth wall. At $y/\delta = 0.15$, $\overline{u^{+2}}$ increases by 18%. For the distribution of $\overline{v^{+2}}$ at the same location, there is an indication that a systematic decrease of approximately 10% exists over the streamwise extent for both surfaces. The collapse of the Reynolds stresses may not be directly related to streamwise independence of the data. A distinction – although difficult to quantify – must be made between the scatter resulting from experimental uncertaincy and a possible streamwise variation. For the rod-roughness, the Reynolds stresses across the inner region of the boundary layer indicate that experimental uncertainty in the data may mask a streamwise dependence. For each Reynolds stress, the errors are discussed with reference to data obtained using X-wires over other wall surfaces.

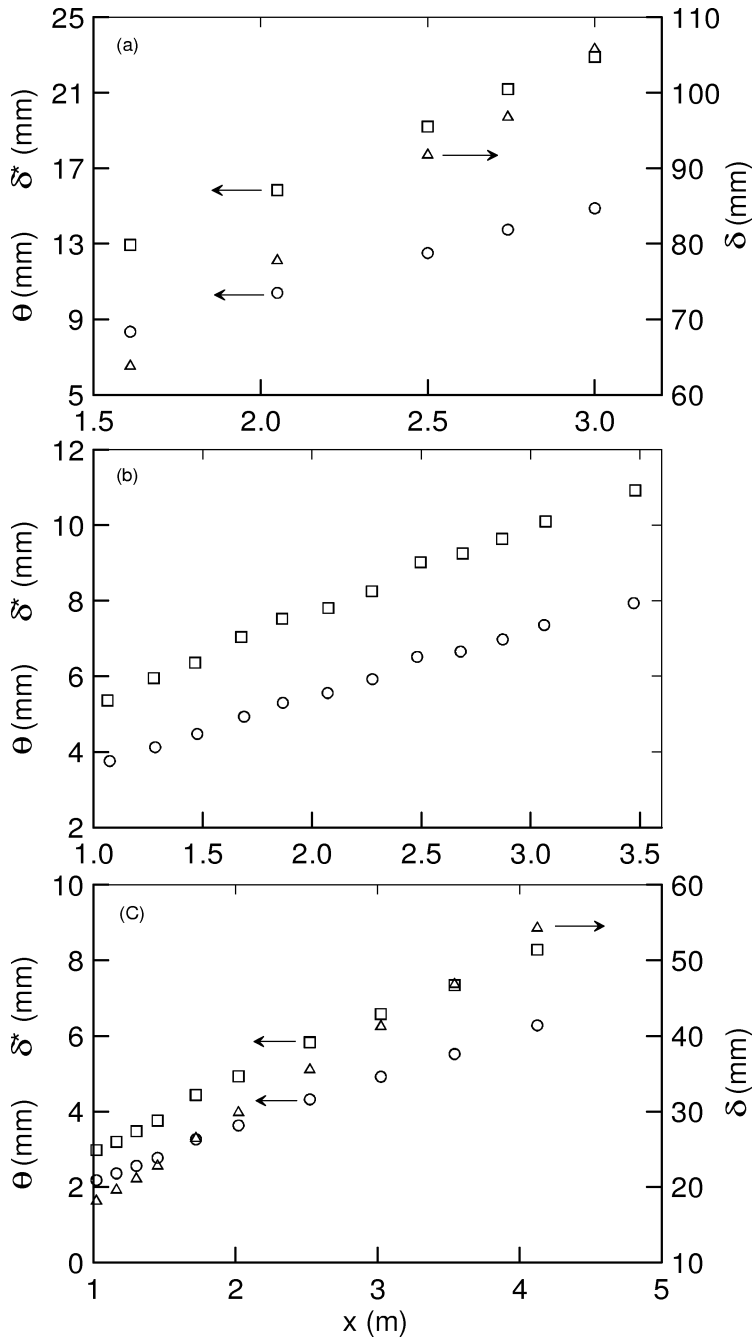

Figure 3. Boundary layer thicknesses. (a) rod-roughness ($5800 \leqslant R_\theta \leqslant 10000$); (b) transverse square cavity [15] ($4000 \leqslant R_\theta \leqslant 8000$); (c) smooth wall [12] ($4900 \leqslant R_\theta \leqslant 10000$), $\square, \delta^*$; Δ, δ; $\bigcirc, \theta$.

5.2. Discussion of Reynolds stress data

The increased scatter for $\overline{u^{+2}}$ and the decrease of $-\overline{u^+v^+}$ as the wall is approached is a consequence of using X-wires in a region in which the local turbulence intensity ($\equiv \overline{u^2}^{1/2}/\overline{U}$) is relatively high. Raupach et

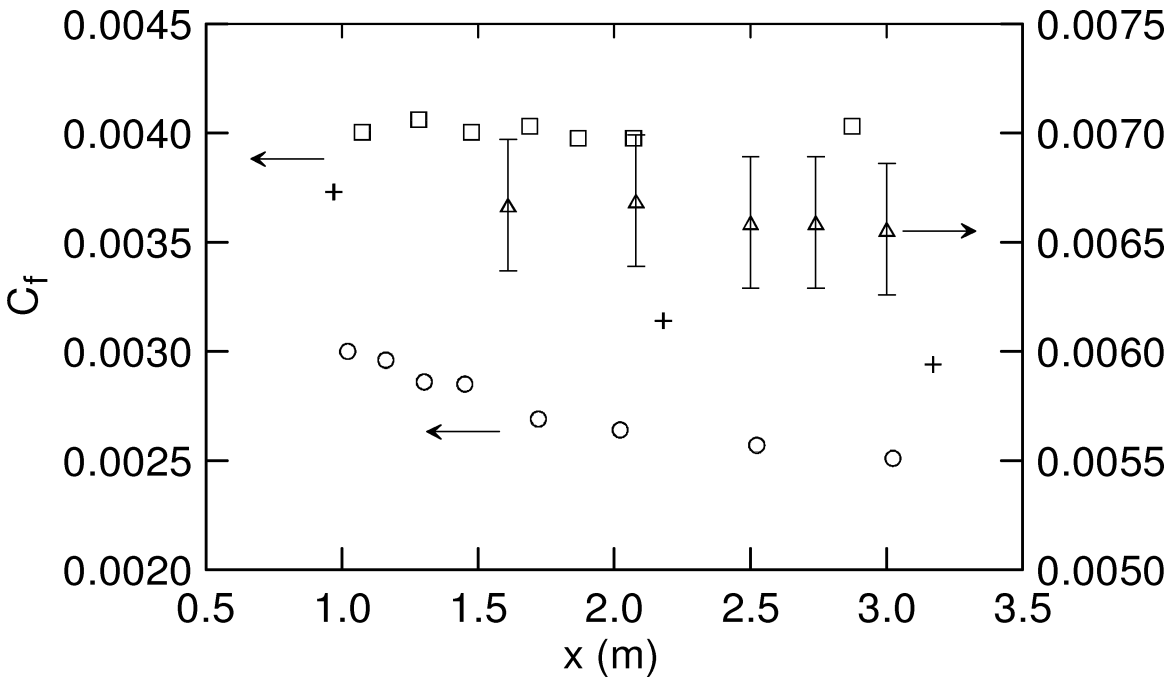

Figure 4. Skin friction, C_f. △, rod-roughness; □, transverse square cavity; + smooth wall [11]; ○, smooth wall [12]. 5% error in the estimation of C_f is shown for the rod-roughness.

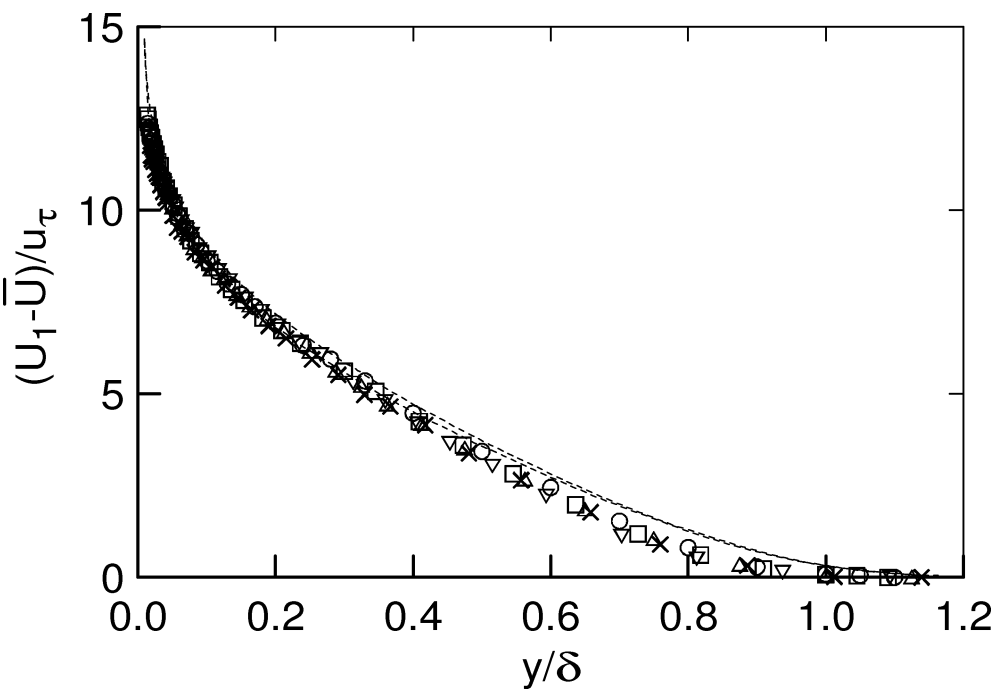

Figure 5. Mean velocity defect for the rod-roughness and a smooth wall. Rod-roughness: ▽, 1.6 m; ×, 2.0 m; △, 2.5 m; ○, 2.7 m; □, 3 m. - - - smooth wall [12]; lower line, $x = 1.1$ m; upper line, $x = 4.1$ m.

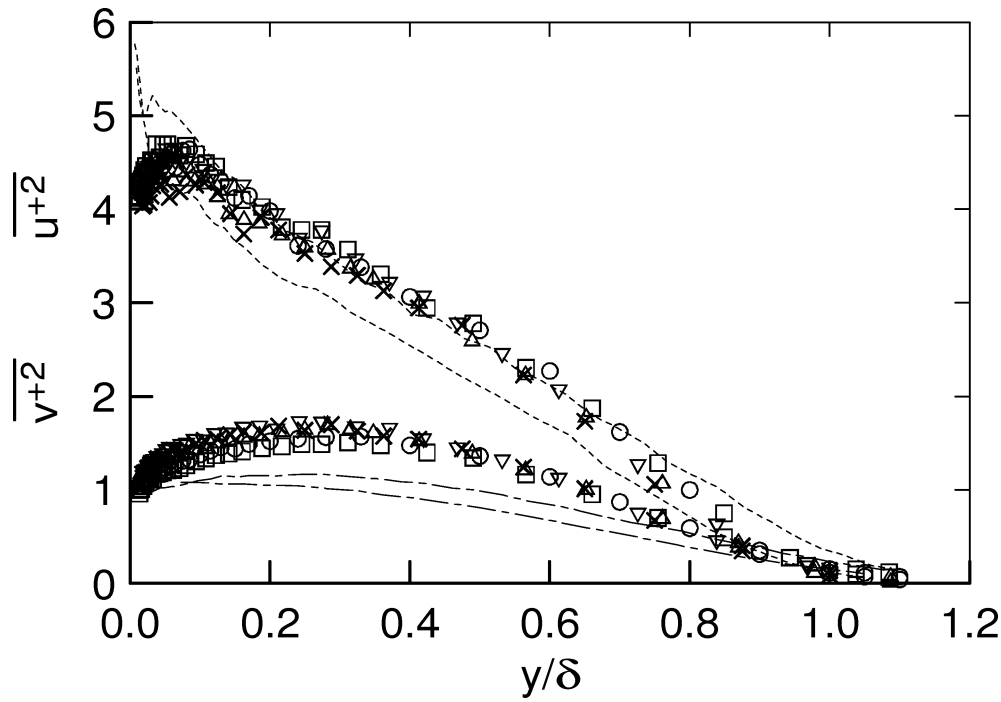

Figure 6. Reynolds stresses for the rod-roughness and a smooth wall. $\overline{u^{+2}}$ and $\overline{v^{+2}}$. Rod-roughness: ▽, 1.6 m; ×, 2.0 m; △, 2.5 m; ○, 2.7 m; □, 3 m. Lines: smooth wall [12]. - - - $\overline{u^{+2}}$; — - — $\overline{v^{+2}}$; lower lines, $x = 1.1$ m; upper lines, $x = 4.1$ m.

al. [28] reviewed X-wire measurement problems in rough wall boundary layers and supported the conclusion of Legg et al. [29], i.e. X-wire measurements of $\overline{u^{+2}}$ and $\overline{v^{+2}}$ are only reliable to an accuracy of 20% when $\overline{u^2}^{1/2}/\overline{U} < 0.35$. For $-\overline{u^+v^+}$, $\overline{u^2}^{1/2}/\overline{U}$ must be less than 0.25. Over a smooth wall, X-wire measurements of the Reynolds stresses may be accurate to within 20% for $y^+ \geqslant 20$, i.e. over nearly the entire boundary layer. This compares with a reduced range, $(y/\delta \geqslant 0.15)$ for the rod-roughness. The Reynolds stresses were corrected for X-wire spatial separation errors using the method in Zhu and Antonia [30]. For data in the near wall region $\overline{u^{+2}}$ may be underestimated by approximately 15%, at $y/\delta = 0.15$, $\overline{u^{+2}}$ was underestimated by 5%.

The decrease of $-\overline{u^+v^+}$ as the wall is approached was also reported and discussed in [31–33] for a square bar roughness with $p/k = 4$ and [34,35] for a wavy wall. For all surfaces, in which measurements were carried out with X-wires, the authors of the cited papers speculated that the decrease of $-\overline{u^+v^+}$ could be due to either X-wire measurements errors or the contribution from a stationary wave to the mean momentum flux, via the term $\langle \overline{U}''\overline{V}'' \rangle$. Here, angular brackets indicate averaging over a streamwise wavelength and a double prime indicates the departure of the time-averaged velocity from the spatially averaged quantity. Over all surfaces, $\langle \overline{U}''\overline{V}'' \rangle$ was negligible relative to $\langle \overline{uv} \rangle$, suggesting that the decrease of $-\overline{u^+v^+}$ is attributed to the use of X-wires in the near-wall region. Using laser doppler velocimetry (LDV) Hudson et al. [36] measured the mean velocity and Reynolds stresses in a channel flow over a wavy wall. They showed that $\langle \overline{U}''\overline{V}'' \rangle$ contributed to τ_w throughout the channel. Djenidi et al. [16], also using LDV over a transverse square bar roughness, reported a non-negligible influence from $\langle \overline{U}''\overline{V}'' \rangle$. Over the latter two surfaces the roughness is relatively large ($h/k = 5$ and $\delta/k = 7$ respectively, where h is the channel half-width), this compares with the data of [31–35], where over these surfaces $\delta/k > 12$ and there was little contribution from $\langle \overline{U}''\overline{V}'' \rangle$. For the rod-roughness surface $\delta/k \simeq 50$.

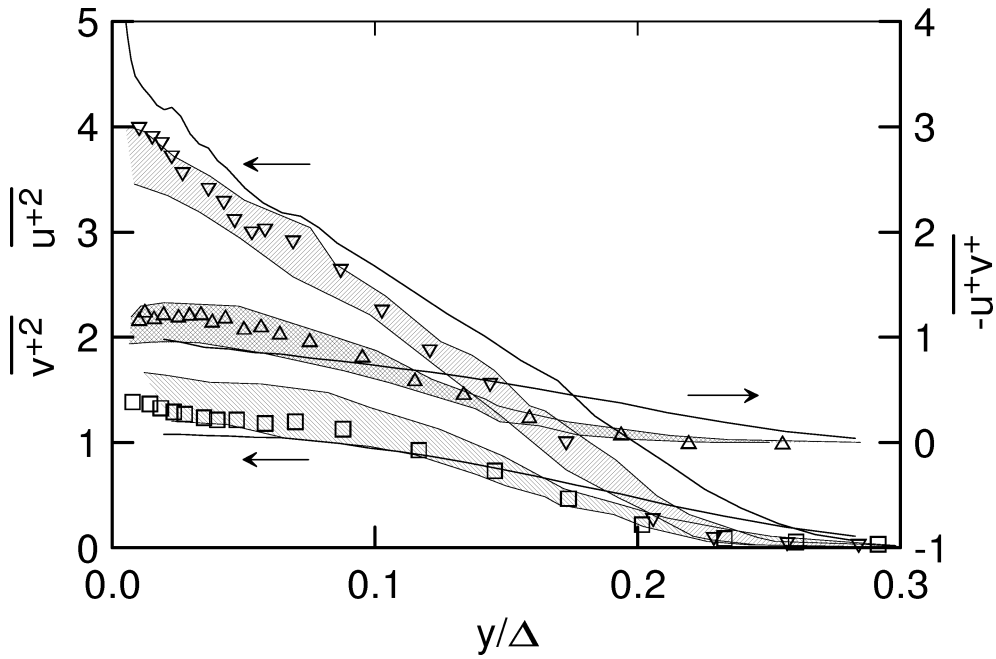

Figure 7. Reynolds stresses for the transverse square cavity roughness and a smooth wall [12]. Hatched region contains the rough wall data of [15] using all streamwise distributions between 1.4 and 3.5 m; symbols, rough wall of [38]. Right hatch, ▽, $\overline{u^{+2}}$; left hatch, □ $\overline{v^{+2}}$; – cross-hatch △, $-\overline{u^+v^+}$. The data of [15] and [38] are from the same set of experiments. Solid lines, smooth wall at $x = 1.1$ m.

Measurement errors in $\overline{v^{+2}}$ have also been previously examined. Antonia [37] compared DNS (direct numerical simulation) data with LDV, particle image velocimetry (PIV) and X-wire measurements of the Reynolds stresses in a smooth wall channel flow. For all quantities, the LDV and PIV measurements agreed well with the DNS data. However, the X-wire distributions of $\overline{v^{+2}}$ were approximately 10% greater, compared with those of the DNS, LDV and PIV distributions. Correcting for errors resulting from the spatial separation of X-wires, $\overline{v^{+2}}$ was overestimated by approximately 5%. Since the presence of the surface roughness influences $\overline{v^{+2}}$ more than the other Reynolds stresses (e.g. Krogstad and Antonia [18]), and the turbulence intensity is higher over rough walls, errors in $\overline{v^{+2}}$, and perhaps $-\overline{u^+v^+}$ would certainly be greater than those in $\overline{u^{+2}}$. Although boundary layer LDV measurements over cylindrical and square bar roughnesses with $p/k = 4$ have not been reported, Reynolds stress measurements close to these walls should be more accurate with LDV than X-wires.

5.3. Additional support for self-preservation

Partial support for self-preservation over a model crop canopy roughness is provided by Raupach et al. [27], who estimated u_τ using the momentum integral method and $-\overline{uv}]^{1/2}_{\text{plateau}}$. They observed a negligible variation of C_f over a streamwise distance of 2 m. Their Reynolds stress data are not normalised and do not provide sufficient indication as to whether equation (1) is satisfied.

The X-wire Reynolds stress data of Osaka et al. [15] for the transverse square cavity are shown in *figure 7*. Since the original data markers in [15] are not individually distinguishable for the 8 streamwise distributions between 1.4 and 3.5 m, hatching is used to indicate the region within which all data lie. One complete Reynolds stress distribution set at $x = 1.8$ m (Kageyama et al. [38]) is also shown. The profiles used are from the data lying within the shaded regions. For rough wall boundary layers, normalisation by Δ is nearly

equivalent to that by δ since $C_f \approx$ const. and $\delta \propto \delta^*$. In contrast with the rod-roughness data, there is increased scatter for the Reynolds stress distribution over the transverse square cavity roughness. The scatter is due to experimental uncertainty using X-wire data, which unfortunately, cannot be quantified. The profiles do not show any systematic variation with x.

While C_f for the transverse square cavity satisfies the self-preservation condition more closely than that for rod-roughness, the Reynolds stresses for the cavity roughness show less collapse. It is not possible to adequately distinguish which rough surface satisfies self-preservation more closely. However both are more self-preserving than a smooth wall. The data presented here indicate that if self-preservation, as defined by equation (1), is to be achieved exactly, then equations (1), (5) and (6) are all required to be satisified.

Analysis of the turbulence structure may provide support for rough wall self-preservation. Based on near-wall flow dynamics, Liu et al. [19], Furuya et al. [20] and Krogstad and Antonia [18], among others, have shown that ejections, sweeps and outward interactions are greater over rough walls compared with smooth wall layers. Djenidi et al. [16] proposed that the mixing helps to maintain the energy equilibrium via a continuous exchange of momentum beween the cavities and the overlying flow. At sufficiently high R_θ, and when $k \ll \delta$ for a fully rough wall, τ_p is likely to be constant with x. It would be worthwhile comparing the streamwise variation of drag-balance estimates of τ_w and τ_p between different rough surfaces, including the present rod-roughness.

6. Conclusions

X-wire measurements were carried out in a turbulent boundary layer over a rod-roughened wall to establish how well self-preservation is approximated, relative to a smooth wall layer. The mean velocity, Reynolds stress and C_f distributions were compared with previous measurements over a transverse square cavity roughness and a smooth wall. It was found that smooth wall layers do not conform as well to self-preservation compared with rough wall layers. The assessment of self-preservation was based on two conditions, $\mathrm{d}\delta/\mathrm{d}x = \text{const.}$ and $\mathrm{d}u_\tau/\mathrm{d}x = 0$, these are obtained from the boundary layer equations at high Reynolds number without assuming a specific form for the mean velocity distribution or a particular roughness geometry. It was, however, suggested that a more accurate test for self-preservation may be possible if a roughness geometry parameter is included in the self-preservation analysis.

Acknowledgements

The authors wish to acknowledge P.-Å. Krogstad for providing helpful comments. The support of the Australian Research Council is gratefully acknowledged.

References

[1] Clauser F.H., Turbulent boundary layers in adverse pressure gradients, J. Aeronaut. Sci. (1954) 91–108.
[2] Clauser F.H., The turbulent boundary layer, Adv. Appl. Mech. 4 (1956) 1–51.
[3] Townsend A.A., The properties of equilibrium boundary layers, J. Fluid Mech. 1 (1956) 561–573.
[4] Townsend A.A., Structure of Turbulent Shear Flows, Cambridge University Press, 1956.
[5] Townsend A.A., Equilibrium layers and wall turbulence, J. Fluid Mech. 11 (1961) 97–120.
[6] Rotta J.C., Turbulent boundary layers in incompressible flow, Prog. Aeronaut. Sci. 2 (1962) 1–219.
[7] Mellor G.L., Gibson D.M., Equilibrium turbulent boundary layers, J. Fluid Mech. 24 (1966) 225–253.
[8] Herring H.J., Norbury J.F., Some experiments on equilibrium turbulent boundary layers in favourable pressure gradients, J. Fluid Mech. 27 (1967) 541–549.
[9] Bradshaw P., The turbulent structure of equilibrium boundary layers, J. Fluid Mech. 29 (1967) 625–645.
[10] Tani I., Some equilibrium turbulent boundary layers, Fluid Dyn. Res. 1 (1986) 49–58.

[11] Osaka H., Kameda T., Mochizuki S., Re-examination of the Reynolds-number-effect on the mean flow quantities in a smooth wall turbulent boundary layer, JSME Int. J. B. 41 (1998) 123–129.
[12] Smith R.W., Effect of Reynolds number on the structure of turbulent boundary layers, PhD thesis, Princeton University, 1994.
[13] Perry A.E., Schofield W.H., Joubert P.N., Rough wall turbulent boundary layers, J. Fluid Mech. 37 (1969) 383–413.
[14] Wood D.H., Antonia R.A., Measurements in a turbulent boundary layer over a *d*-type surface roughness, J. Appl. Mech. 42 (1975) 591–597.
[15] Osaka H., Nishino T., Oyama S., Kageyama Y., Self-preservation for a turbulent boundary layer over a *d*-type rough surface, Mem. Fac. Eng. Yamaguchi University 33 (1982) 9–16.
[16] Djenidi L., Elavarasan R., Antonia R.A., The turbulent boundary layer over transverse square cavity, J. Fluid Mech. 395 (1999) 271–294.
[17] Liu C.Y., Huang M.Y., Experimental study of turbulent boundary layer along a flat plate with linear increase of roughness height, Aeronaut. J. 77 (1973) 192–193.
[18] Krogstad P.-Å., Antonia R.A., Effect of surface conditions on a turbulent boundary layer, Exp. Fluids 27 (1999) 450–460.
[19] Liu C.K., Kline S.J., Johnston J., An experimental study of turbulent boundary layer on rough walls, Tech. Rep. MD-15, Department of Mechanical Engineering, Stanford University, 1966.
[20] Furuya Y., Miyata M., Fujita H., Turbulent boundary layer and flow resistance on plates roughened by wires, J. Fluids Eng. 98 (1976) 635–644.
[21] Hosni M.H., Coleman H.W., Taylor R.P., Measurements and calculations of fluid dynamic characteristics of rough-wall turbulent boundary layers, J. Fluids Eng. 115 (1993) 383–388.
[22] Ranga Raju K.G., Loeser J., Plate E.J., Velocity profiles and fence drag for a turbulent boundary layer along smooth and rough flat plates, J. Fluid Mech. 76 (1976) 383–399.
[23] Bandyopadhyay P.R., Rough-wall turbulent boundary layers in the transition regime, J. Fluid Mech. 180 (1987) 231–266.
[24] Krogstad P.-Å., Antonia R.A., Browne L.W.B., Comparison between rough- and smooth-wall turbulent boundary layers, J. Fluid Mech. 245 (1992) 599–617.
[25] Browne L.W.B., Antonia R.A., Chua L.P., Calibration of X-probes for turbulent flow measurements, Exp. Fluids 7 (1989) 201–208.
[26] Weber R.O., Remarks on the definition and estimation of friction velocity, Boundary-Layer Meteorol. 93 (1999) 197–209.
[27] Raupach M.R., Coppin P.A., Legg B.J., Experiments on scalar dispersion within a model plant canopy. Part 1: The turbulence structure, Boundary-Layer Meteorol. 35 (1986) 21–52.
[28] Raupach M.R., Antonia R.A., Rajagopalan S., Rough-wall turbulent boundary layers, Appl. Mech. Rev. 44 (1991) 1–25.
[29] Legg B.J., Coppin P.A., Raupach M.R., A three-hot-wire anemometer for measuring two velocity components in high intensity turbulent boundary layers, J. Phys. E: Sci. Instrum. 17 (1984) 970–976.
[30] Zhu Y., Antonia R.A., Effect of wire separation on X-probe measurements in a turbulent boundary layer, J. Fluid Mech. 287 (1995) 199–223.
[31] Antonia R.A., Luxton R.E., The response of a turbulent boundary layer to a change in surface roughness. Part 2. Rough to smooth, J. Fluid Mech. 53 (1971) 736–757.
[32] Mulhearn P.J., Turbulent flow over a periodic rough surface, Phys. Fluids 21 (1978) 1113–1115.
[33] Kameda T., Osaka H., Mochizuki S., Mean flow quantities for the turbulent boundary layer over a *k*-type rough wall, in: Thomson M.C., Hourigan K. (Eds.), 13th Australasian Fluid Mechanics Conference, Monash University, Melbourne, 1998, pp. 357–360.
[34] Perry A.E., Lim K.L., Henbest S.M., An experimental study of the turbulence structure in smooth- and rough-wall boundary layers, J. Fluid Mech. 177 (1987) 437–466.
[35] Gong W., Taylor P.A., Dörnbrack A., Turbulent boundary-layer flow over fixed aerodynamically rough two-dimensional sinusoidal waves, J. Fluid Mech. 312 (1996) 1–37.
[36] Hudson J.D., Dykhno L., Hanratty T.J., Turbulence production in flow over a wavy wall, Exp. Fluids 20 (1996) 257–265.
[37] Antonia R.A., Direct numerical simulations and hot wire experiments: A possible way ahead?, in: Dracos T., Tsinober A. (Eds.), New Approaches and Concepts in Turbulence, Basel, 1993, pp. 347–365.
[38] Kageyama Y., Osaka H., Nishino T., Turbulence quantites of a turbulent boundary layer over a *d*-type rough surface, Mem. Fac. Eng. Yamaguchi University 33 (1982) 17–24.